EUROPEAN JOURNAL OF BIOMEDICAL AND PHARMACEUTICAL SCIENCES
http://www.ejbps.com

ISSN 2349-8870
Volume: 11
Issue: 8
138-150
Year: 2024

MATHEMATICAL TREATMENT OF WHITE NOISE IMPACT ON COVID-19 DISEASE TRANSMISSION MODEL UNDER QUARANTINE STRATEGY

Y. Divya Lakshmi[1], J. Praveshika[2], M. N. Srinivas[3]*, B. S. N. Murthy[4] and V. Madhusudanan[5]

[1,2,3]Department of Mathematics, School of Advanced Sciences, Vellore Institute of Technology, Vellore-632014, Tamil Nadu, India.
[4]Department of Mathematics, Aditya College of Engineering and Technology, Surampalem, India.
[5]Department of Mathematics, S.A. Engineering College, Chennai 600077, Tamil Nadu, India.

***Corresponding Author: M. N. Srinivas**
Department of Mathematics, School of Advanced Sciences, Vellore Institute of Technology, Vellore-632014, Tamil Nadu, India.

Article Received on 13/06/2024 **Article Revised on 03/07/2024** **Article Accepted on 23/07/2024**

ABSTRACT
In this article, we provide a mathematical model that depicts the dynamics of the COVID-19 illness while incorporating vaccination measures and quarantine measures. The interaction between the susceptible, exposed, infected, vaccinated, and recovered individuals is described by five equations in the SLIVR model that is being given. To understand and analyse the stochastic stability of this system, Fourier transform is used and numerical simulations are conducted to show how the infection behaves over time and how vaccination and quarantine affects the dynamics of COVID-19. MATLAB is used to provide the graphical understanding about the steadiness.

KEYWORDS: Stability, susceptible, exposed, infected, vaccination, recovered, epidemic model, quarantine measure, COVID-19.

1. INTRODUCTION
The World Health Organization (WHO) received its first report on December 31, 2019, regarding a cluster of cases that resembled viral pneumonia in Wuhan, China. COVID-19 is a disease caused by the SARS-CoV-2 virus. As the illness spread rapidly throughout China and the rest of the world, it became a serious global issue. COVID-19 was declared as a pandemic by the World Health Organization (WHO) on March 11, 2020 it also published the preliminary guidelines to be followed to control the pandemic in countries affected.[1] Individuals can contract the virus directly from infected surfaces or through direct touch. Common symptoms include fevers and sore throats, but it may additionally trigger less common symptoms like exhaustion, muscle aches, and respiratory issues[2] Numerous infectious case reports and fatalities were made. Human progress persists even in the face of devastating calamities. Throughout history, a great deal of serious infectious diseases has claimed a great deal of lives, significantly more than have been claimed by global conflicts. In relation to control and prediction about the dynamics of various diseases[3,4,5,6,7,8,9] mathematical modelling in epidemiology is a useful tool.[10] Many countries are affected due to this pandemic and mathematical modelling helps in understanding the pandemic better in various Communities.[11,12]

Researchers from all over the world are actively investigating several epidemic models that have been applied to the propagation of COVID-19. Ian et al[13] devised a susceptible-infected-removed (SIR) model, offering a theoretical framework for studying the temporal progression of diverse populations and monitoring key crucial parameters for the COVID-19 disease's spread in different communities. Additionally, the SARS-COV-2 virus is characterized by a prolonged incubation period, referring to the period between virus exposure and development of symptoms. There are documented ranges of 2 to 27 days during the incubation phase, with an average duration of 6 days.[14] Many earlier scholars suggested expanding the classic SIR model by including a new compartment for the population who are exposed. Shaobo et al.[15] applied SLIR model for the analysis of COVID-19 epidemic outbreak in Hubei Province. Furthermore, a multitude of mathematical models have been developed to examine the COVID-19 epidemic across different countries.[16,17,18,19]

Early identification methods, medical treatment to decrease the count of infected individuals and social distancing[20] to reduce personal contact are just a few of the stringent and sufficient measures implemented globally for the prevention and control of the spread of COVID-19[21,22] The management of COVID-19 involves

the use of immunization and isolation.[23,24] One important strategy in the fight against several long-standing diseases is the use of vaccinations. Authors in[25] have developed a SLIR model incorporating isolation and vaccination as model parameters[26] Amouch et al introduced a new epidemiology mathematical model to comprehend the transmission dynamics of COVID-19,[27] it focus on the transmission dynamics of individuals exhibiting severe, mild, and asymptomatic symptoms as well as accounting for certain susceptible individuals' vaccination history. A recent study looked at an epidemic model of the COVID-19 vaccination.[28] In this work, we further investigate the vaccination effects by examining the influence of quarantine on the SLIVR COVID-19 epidemic model from[28] Consequently, the second portion of the SLIVR COVID-19 pandemic model is constructed as follows.

The structure of this work is as follows: In section 2, mathematical model is created for the susceptible-exposed-infected-vaccinated-recovered population. In section 3 dynamical behaviour of the system with noise is given. Section 4 contains the numerical simulations and the graphs to show the steadiness of the system. Section 5 contains the observations about the model. Section 6 is the conclusion section.

2. Noise Formulation of Covid-19 Disease Transmission on S-L-I-V-R Model

This SLIVR epidemic model was created using the following components: susceptible individuals (*S*), the population that can become infected, Individuals who have been exposed (*L*), and the population segment that has encountered the virus but remains asymptomatic with coronavirus symptoms in complete development, or the infectious individuals (*I*). Both the vaccinated (*V*) and, eventually, the recovered(*R*) individuals.

The dynamics of the suggested model are represented by the system of nonlinear differential equations with noise that follows. Details about the configuration of the system are given in Table 1.

$$\left.\begin{aligned} S'(\mathrm{t}) &= A - \alpha(1-\sigma)[\mathrm{I} + \beta L]\left(\frac{S}{N}\right) - (r_0 + d_0)S + r_1 V + r_2 R + \rho_1 \Psi_1(t) \\ L'(\mathrm{t}) &= \alpha(1-\sigma)[I + \beta L]\left(\frac{S}{N}\right) - (d_0 + r_3)S + \rho_2 \Psi_2(t) \\ I'(t) &= r_3 L - (d_0 + d_1 + r_4)I + \rho_3 \Psi_3(t) \\ V'(t) &= r_0 S - (d_0 + r_1)V + \rho_4 \Psi_4(t) \\ R'(\mathrm{t}) &= r_4 I - (d_0 + r_2)R + \rho_5 \Psi_5(t) \end{aligned}\right\} \quad (2.1)$$

Table 1

Parameter	Description of the parameters	Value
A	Population recruitment rate	25
α	Effective contact rate	0.15
β	Relative transmissibility rate	0.05
σ	The effective of quarantine in decreasing the number of people with latent or active infections	0.1
r_0	Vaccination rate	0.01
r_1	Vaccine waning rate	0.02
r_2	Loss of disease acquired immunity	0.03
r_3	Rate of infection development with symptoms	0.04
r_4	Rate of recovery from infection	0.05
d_0	Natural mortality	0.3
d_1	Death rate due to infection	0.2
N	Population rate	100

The parameter signifies the effectiveness of quarantine in decreasing the number of individuals who are carrying the virus but not yet showing symptoms, as well as those who are already infected. The diagram outlining our model is depicted hereafter are already infected.

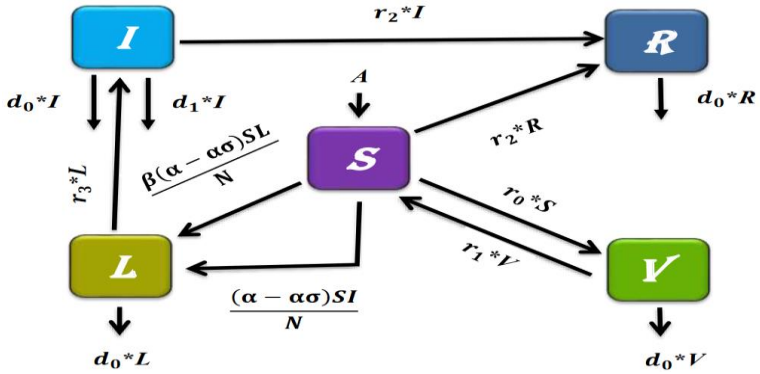

Fig. 1: The flow chart of the Covid-19 disease transmission.

3. Analysis of White Noise on Covid-19 Disease Transmission

Climate and natural disturbances are two examples of the many forces that give ecological systems distinctive characteristics. These forces are not consistent across time. Given the unpredictability of climatic variations, weather patterns, and sporadic disruptions like fires, landslides, and earthquakes, Aside from processes driven by deterministic oscillations, a large amount of environmental variability is random, such as insect outbreaks and so forth. It is motivated to investigate how a stochastic setting could modify and characterize the behaviour of natural systems because random drivers are present in bio-geophysical processes.[29] We will now examine the stochastic models to demonstrate how random environmental variables affect stability (2.1). Because of random fluctuations, the model's parameters fluctuate around their average values. We examine the randomness of additive white noises**.** We take into account the model's randomness (2.1). The perturbation of white noise will alter any parameter in the model a $\rho_i \Psi_i(t)$ where $\Psi_i(t)$denotes a Gaussian white noise occurring at a particular time instance t and ρ_i is the noise amplitude. In contrast, the equilibrium states of the deterministic and stochastic models are the same and will now fluctuate about their mean states.

We analyse model dynamics (1) around the interior equilibrium point $\tilde{P}(S^*, L^*, I^*, V^*, R^*)$.Let

$S(t)=h_1(t)+S^*; L(t)=h_2(t)+L^*; I(t)=h_3(t)+I^*; V(t)=h_4(t)+V^*; R(t)=h_5(t)+R^*$ (3.1)

$S'(t)=h_1'(t);\ L'(t)=h_2'(t);\ I'(t)=h_3'(t);\ V'(t)=h_4'(t);\ R'(t)=h_5'(t)$ (3.2)

and by concentrating just on the consequences of stochastic linear perturbations. Using (3.1) and (3.2);

$$h_1'(t) = A-(\alpha-\sigma\alpha)[(h_3(t)+I^*)+\beta(h_2(t)+L^*)]\frac{h_1(t)+S^*}{N}-(r_0+d_0)(h_1(t)+S^*)+ r_1(h_4(t)+V^*)+r_2(h_5(t)+R^* \quad (3.2)$$

$+\rho_1\Psi_1(t)$ (3.3)

$$h_2'(t) = (\alpha-\sigma\alpha)[(h_3(t)+I^*)+\beta(h_2(t)+L^*)]\frac{h_1(t)+S^*}{N}-(d_0+r_3)(h_2(t)+L^*)+ \rho_2\Psi_2(t) \quad (3.4)$$

$h_3'(t) = r_3(h_2(t)+L^*)-(d_0+d_1+r_4)(h_3(t)+I^*)+\rho_3\Psi_3(t)$ (3.5)

$h_4'(t) = r_0(h_1(t)+S^*)-(d_0+r_1)(h_4(t)+V^*)+\rho_4\Psi_4(t)$ (3.6)

$h_5'(t) = r_4(h_3(t)+I^*)-(d_0+r_2)(h_5(t)+R^*)+\rho_5\Psi_5(t)$ (3.7)

Model (2.1) is therefore condensed to the simple linear arrangement illustrated below.

$h_1'(t) = \frac{-(\alpha-\sigma\alpha)}{N}[S^*h_3+\beta S^*h_2]+\rho_1\Psi_1(t)$ (3.8)

$h_2'(t) = \frac{\beta(\alpha-\sigma\alpha)}{N}[L^*h_1]+\rho_2\Psi_2(t)$ (3.9)

$h_3'(t) = \rho_3\Psi_3(t)$ (3.10)

$h_4'(t) = \rho_4\Psi_4(t)$ (3.11)

$h_5'(t) = \rho_5\Psi_5(t)$ (3.12)

Taking Fourier transform for (3.6)-(3.10) we get,

$\rho_1\widetilde{\Psi_1}(\omega) = (i\omega)\widetilde{h_1}(\omega)+\frac{(\alpha-\sigma\alpha)}{N}[S^*h_3(\omega)+\beta S^*h_2]$ (3.13)

$$\rho_{2\tilde{\Psi}_2}(\omega) = (i\omega)\widetilde{h_2}(\omega) - \frac{\beta(\alpha-\sigma\alpha)}{N}[L^*\widetilde{h_1}(\omega)] \quad (3.14)$$

$$\rho_{3\tilde{\Psi}_3}(\omega) = (i\omega)\widetilde{h_3}(\omega) \quad (3.15)$$

$$\rho_{4\tilde{\Psi}_4}(\omega) = (i\omega)\widetilde{h_4}(\omega) \quad (3.16)$$

$$\rho_{5\tilde{\Psi}_5}(\omega) = (i\omega)\widetilde{h_5}(\omega) \quad (3.17)$$

The matrix form of the equations (3.13)-(3.17) as

$$P(\omega)\tilde{h}(\omega) = \tilde{\Psi}(\omega) \quad (3.18)$$

Where $P(\omega) = \begin{bmatrix} a_1 & b_1 & c_1 & d_1 & e_1 \\ a_2 & b_2 & c_2 & d_2 & e_2 \\ a_3 & b_3 & c_3 & d_3 & e_3 \\ a_4 & b_4 & c_4 & d_4 & e_4 \\ a_5 & b_5 & c_5 & d_5 & e_5 \end{bmatrix}$

$$\tilde{h}(\omega) = [\widetilde{h_1}(\omega), \widetilde{h_2}(\omega), \widetilde{h_3}(\omega), \widetilde{h_4}(\omega), \widetilde{h_5}(\omega)]^T;$$

$$\tilde{\Psi}(\omega) = [\rho_{1\tilde{\Psi}_1}(\omega), \rho_{2\tilde{\Psi}_2}(\omega), \rho_{3\tilde{\Psi}_3}(\omega), \rho_{4\tilde{\Psi}_4}(\omega), \rho_{5\tilde{\Psi}_5}(\omega)]^T;$$

$$a_1 = i\omega; b_1 = \frac{\beta(\alpha-\sigma\alpha)}{N}S^*; c_1 = \frac{(\alpha-\sigma\alpha)}{N}S^*; d_1 = 0; e_1 = 0;$$

$$a_2 = -\frac{\beta(\alpha-\sigma\alpha)}{N}L^*; b_2 = i\omega; c_2 = 0; d_2 = 0; e_2 = 0;$$

$$a_3 = 0; b_3 = 0; c_3 = i\omega; d_3 = 0; e_3 = 0;$$

$$a_4 = 0; b_4 = 0; c_4 = 0; d_4 = i\omega; e_4 = 0;$$

$$a_5 = 0; b_5 = 0; c_5 = 0; d_5 = 0; e_5 = i\omega;$$

$$= \begin{bmatrix} i\omega & \beta\frac{(\alpha-\sigma\alpha)}{N}S^* & \frac{(\alpha-\sigma\alpha)}{N}S^* & 0 & 0 \\ -\beta\frac{(\alpha-\sigma\alpha)}{N}L^* & i\omega & 0 & 0 & 0 \\ 0 & 0 & i\omega & 0 & 0 \\ 0 & 0 & 0 & i\omega & 0 \\ 0 & 0 & 0 & 0 & i\omega \end{bmatrix}$$

$$|P(\omega)| = c_3 d_4 e_5 [a_1 b_2 - a_2 b_1]$$

$$|P(\omega)| = (i\omega)^3 * \{(i\omega)^2 + [\frac{(\alpha-\sigma\alpha)}{N}]^2\beta^2 S^* L^*\}$$

adj[P(ω)]=

$$\begin{bmatrix} b_2c_3d_4e_5 & -b_1c_3d_4e_5 & -b_2c_1d_4e_5 & 0 & 0 \\ -a_2c_3d_4e_5 & a_1c_3d_4e_5 & a_2c_1d_4e_5 & 0 & 0 \\ 0 & 0 & d_4e_5[a_1b_2 - a_2b_1] & 0 & 0 \\ 0 & 0 & 0 & c_3e_5[a_1b_2 - a_2b_1] & 0 \\ 0 & 0 & 0 & 0 & c_3d_4[a_1b_2 - a_2b_1] \end{bmatrix}$$

As an alternative, equation (3.16) can be expressed as

$$\tilde{h}(\omega) = [P(\omega)]^{-1}\tilde{\Psi}(\omega) \quad (3.19)$$

$$[P(\omega)]^{-1} = Q(\omega) \quad (3.20)$$

Where $Q(\omega) = \frac{adj[P(\omega)]}{|P(\omega)|}$ (3.21)

$$Q = \frac{1}{|P(\omega)|}\begin{bmatrix} a_{11} & a_{12} & a_{13} & a_{14} & a_{15} \\ b_{11} & b_{12} & b_{13} & b_{14} & b_{15} \\ c_{11} & c_{12} & c_{13} & c_{14} & c_{15} \\ d_{11} & d_{12} & d_{13} & d_{14} & d_{15} \\ e_{11} & e_{12} & e_{13} & e_{14} & e_{15} \end{bmatrix}$$

$a_{11} = (i\omega)^4$; $a_{12} = -\beta\frac{(\alpha-\sigma\alpha)}{N}S^*(i\omega)^3$; $a_{13} = -\frac{(\alpha-\sigma\alpha)}{N}S^*(i\omega)^3$; $a_{14} = 0$; $a_{15} = 0$;

$b_{11}=\frac{\beta(\alpha-\sigma\alpha)}{N}L^*\,(i\omega)^3$; $b_{12}=(i\omega)^4$;$b_{13}=-\beta\left[\frac{(\alpha-\sigma\alpha)}{N}\right]^2 S^*L^*\,(i\omega)^2$; $b_{14}=0$; $b_{15}=0$; $c_{11}=0$; $c_{12}=0$;

$c_{13}=(i\omega)^4+(i\omega)^2\beta^2\left[\frac{(\alpha-\sigma\alpha)}{N}\right]^2 S^*L^*$; $c_{14}=0$; $c_{15}=0$;$d_{11}=0$; $d_{12}=0$; $d_{13}=0$;

$d_{14}=(i\omega)^4+(i\omega)^2\beta^2\left[\frac{(\alpha-\sigma\alpha)}{N}\right]^2 S^*L^*$; $d_{15}=0$;$e_{11}=0$; $e_{12}=0$; $e_{13}=0$; $e_{14}=0$;

$e_{15}=(i\omega)^4+(i\omega)^2\beta^2\left[\frac{(\alpha-\sigma\alpha)}{N}\right]^2 S^*L^*$

The variations in the intensity of the variable, denoted as h_i where i ranges from 1 to 5, are provided.

$\sigma_{h_i}^2=\frac{1}{2\pi}\sum_{i=1}^{5}\int_{-\infty}^{\infty}\propto_i\left|Q_{ij}(\omega)\right|^2 d\omega$; i =1, 2,3,4,5

Variance of h_i , i =1,2,3,4,5 are calculated as

$$\sigma_{h_1}^2=\frac{1}{2\pi}\int_{-\infty}^{\infty}\propto_1\left|\frac{a_{11}}{|P(\omega)|}\right|^2 d\omega+\int_{-\infty}^{\infty}\propto_2\left|\frac{a_{12}}{|P(\omega)|}\right|^2 d\omega+\int_{-\infty}^{\infty}\propto_3\left|\frac{a_{13}}{|P(\omega)|}\right|^2 d\omega+\int_{-\infty}^{\infty}\propto_4\left|\frac{a_{14}}{|P(\omega)|}\right|^2 d\omega+\int_{-\infty}^{\infty}\propto_5\left|\frac{a_{15}}{|P(\omega)|}\right|^2 d\omega$$

$$\sigma_{h_1}^2=\frac{1}{2\pi}\int_{-\infty}^{\infty}\propto_1\left|\frac{(i\omega)^4}{|P(\omega)|}\right|^2 d\omega+\int_{-\infty}^{\infty}\propto_2\left|\frac{\frac{-\beta(\alpha-\sigma\alpha)}{N}S^*\,(i\omega)^3}{|P(\omega)|}\right|^2 d\omega+\int_{-\infty}^{\infty}\propto_3\left|\frac{-\frac{(\alpha-\sigma\alpha)}{N}S^*\,(i\omega)^3}{|P(\omega)|}\right|^2 d\omega \quad (3.22)$$

$$\sigma_{h_2}^2=\frac{1}{2\pi}\int_{-\infty}^{\infty}\propto_1\left|\frac{b_{11}}{|P(\omega)|}\right|^2 d\omega+\int_{-\infty}^{\infty}\propto_2\left|\frac{b_{12}}{|P(\omega)|}\right|^2 d\omega+\int_{-\infty}^{\infty}\propto_3\left|\frac{b_{13}}{|P(\omega)|}\right|^2 d\omega+\int_{-\infty}^{\infty}\propto_4\left|\frac{b_{14}}{|P(\omega)|}\right|^2 d\omega+\int_{-\infty}^{\infty}\propto_5\left|\frac{b_{15}}{|P(\omega)|}\right|^2 d\omega$$

$$\sigma_{h_2}^2=\frac{1}{2\pi}\int_{-\infty}^{\infty}\propto_1\left|\frac{\frac{\beta(\alpha-\sigma\alpha)}{N}L^*\,(i\omega)^3}{|P(\omega)|}\right|^2 d\omega+\int_{-\infty}^{\infty}\propto_2\left|\frac{(i\omega)^4}{|P(\omega)|}\right|^2 d\omega+\int_{-\infty}^{\infty}\propto_3\left|\frac{\frac{\beta(\alpha-\sigma\alpha)^2}{N^2}S^*L^*\,(i\omega)^2}{|P(\omega)|}\right|^2 d\omega \quad (3.23)$$

$$\sigma_{h_3}^2=\frac{1}{2\pi}\int_{-\infty}^{\infty}\propto_1\left|\frac{c_{11}}{|P(\omega)|}\right|^2 d\omega+\int_{-\infty}^{\infty}\propto_2\left|\frac{c_{12}}{|P(\omega)|}\right|^2 d\omega+\int_{-\infty}^{\infty}\propto_3\left|\frac{c_{13}}{|P(\omega)|}\right|^2 d\omega+\int_{-\infty}^{\infty}\propto_4\left|\frac{c_{14}}{|P(\omega)|}\right|^2 d\omega+\int_{-\infty}^{\infty}\propto_5\left|\frac{c_{15}}{|P(\omega)|}\right|^2 d\omega$$

$$\sigma_{h_3}^2=\frac{1}{2\pi}\int_{-\infty}^{\infty}\propto_3\left|\frac{(i\omega)^4+(i\omega)^2\frac{\beta^2(\alpha-\sigma\alpha)^2}{N^2}S^*L^*}{|P(\omega)|}\right|^2 d\omega \quad (3.24)$$

$$\sigma_{h_4}^2=\frac{1}{2\pi}\int_{-\infty}^{\infty}\propto_1\left|\frac{d_{11}}{|P(\omega)|}\right|^2 d\omega+\int_{-\infty}^{\infty}\propto_2\left|\frac{d_{12}}{|P(\omega)|}\right|^2 d\omega+\int_{-\infty}^{\infty}\propto_3\left|\frac{d_{13}}{|P(\omega)|}\right|^2 d\omega+\int_{-\infty}^{\infty}\propto_4\left|\frac{d_{14}}{|P(\omega)|}\right|^2 d\omega+\int_{-\infty}^{\infty}\propto_5\left|\frac{d_{15}}{|P(\omega)|}\right|^2 d\omega$$

$$\sigma_{h_4}^2=\frac{1}{2\pi}\int_{-\infty}^{\infty}\propto_4\left|\frac{(i\omega)^4+(i\omega)^2\frac{\beta^2(\alpha-\sigma\alpha)^2}{N^2}S^*L^*}{|P(\omega)|}\right|^2 d\omega \quad (3.25)$$

$$\sigma_{h_5}^{\,2} = \frac{1}{2\pi}\int_{-\infty}^{\infty} \propto_1 \left|\frac{e_{11}}{|\mathrm{P}(\omega)|}\right|^2 d\omega + \int_{-\infty}^{\infty} \propto_2 \left|\frac{e_{12}}{|\mathrm{P}(\omega)|}\right|^2 d\omega + \int_{-\infty}^{\infty} \propto_3 \left|\frac{e_{13}}{|\mathrm{P}(\omega)|}\right|^2 d\omega + \int_{-\infty}^{\infty} \propto_4 \left|\frac{e_{14}}{|\mathrm{P}(\omega)|}\right|^2 d\omega + \int_{-\infty}^{\infty} \propto_5 \left|\frac{e_{15}}{|\mathrm{P}(\omega)|}\right|^2 d\omega$$

$$\sigma_{h_5}^{\,2} = \frac{1}{2\pi}\int_{-\infty}^{\infty} \propto_5 \left|\frac{(i\omega)^4 + (i\omega)^2 \frac{\beta^2(\alpha-\sigma\alpha)^2}{N^2} S^* L^*}{|\mathrm{P}(\omega)|}\right|^2 d\omega \quad (3.26)$$

From (3.20)-(3.24) we get,

$$\sigma_{h_1}^{\,2} = \frac{1}{2\pi}\int_{-\infty}^{\infty} \frac{\propto_1 [\omega^4]^2 + \propto_2 \left[\frac{\beta(\alpha-\sigma\alpha)}{N} S^* i\omega^3\right]^2 + \propto_3 \left[\frac{(\alpha-\sigma\alpha)}{N} S^* i\omega^3\right]^2}{\left[i\omega^5 - i\omega^3 \frac{\beta^2(\alpha-\sigma\alpha)^2}{N^2} S^* L^*\right]^2} d\omega \quad (3.27)$$

$$\sigma_{h_2}^{\,2} = \frac{1}{2\pi}\int_{-\infty}^{\infty} \frac{\propto_1 \left[\frac{\beta(\alpha-\sigma\alpha)}{N} L^* i\omega^3\right]^2 + \propto_2 [\omega^4]^2 + \propto_3 \left[\frac{\beta(\alpha-\sigma\alpha)^2}{N^2} S^* L^* \omega^2\right]^2}{\left[i\omega^5 - i\omega^3 \frac{\beta^2(\alpha-\sigma\alpha)^2}{N^2} S^* L^*\right]^2} d\omega \quad (3.28)$$

$$\sigma_{h_3}^{\,2} = \frac{1}{2\pi}\int_{-\infty}^{\infty} \frac{\propto_3 \left[\omega^4 - \omega^2 \frac{\beta^2(\alpha-\sigma\alpha)^2}{N^2} S^* L^*\right]^2}{\left[i\omega^5 - i\omega^3 \frac{\beta^2(\alpha-\sigma\alpha)^2}{N^2} S^* L^*\right]^2} d\omega \quad (3.29)$$

$$\sigma_{h_4}^{\,2} = \frac{1}{2\pi}\int_{-\infty}^{\infty} \frac{\propto_4 \left[\omega^4 - \omega^2 \frac{\beta^2(\alpha-\sigma\alpha)^2}{N^2} S^* L^*\right]^2}{\left[i\omega^5 - i\omega^3 \frac{\beta^2(\alpha-\sigma\alpha)^2}{N^2} S^* L^*\right]^2} d\omega \quad (3.30)$$

$$\sigma_{h_5}^{\,2} = \frac{1}{2\pi}\int_{-\infty}^{\infty} \frac{\propto_5 \left[\omega^4 - \omega^2 \frac{\beta^2(\alpha-\sigma\alpha)^2}{N^2} S^* L^*\right]^2}{\left[i\omega^5 - i\omega^3 \frac{\beta^2(\alpha-\sigma\alpha)^2}{N^2} S^* L^*\right]^2} d\omega \quad (3.31)$$

The system dynamics of (3.6)-(3.10) with either $\propto_1$=0 (or) $\propto_2$=0 (or) $\propto_3$=0 (or) $\propto_4$=0 (or) $\propto_5$=0, then population variance are:

If $\propto_1$=$\propto_2$=$\propto_3$=$\propto_4$=0, then $\sigma_{h_1}^{\,2} = \sigma_{h_2}^{\,2} = \sigma_{h_3}^{\,2} = \sigma_{h_4}^{\,2} = 0$

$$\sigma_{h_5}^{\,2} = \frac{\propto_5}{2\pi}\int_{-\infty}^{\infty} \frac{\left[\omega^4 - \omega^2 \frac{\beta^2(\alpha-\sigma\alpha)^2}{N^2} S^* L^*\right]^2}{\left[i\omega^5 - i\omega^3 \frac{\beta^2(\alpha-\sigma\alpha)^2}{N^2} S^* L^*\right]^2} d\omega \quad (3.32)$$

If $\propto_1$=$\propto_2$=$\propto_3$=$\propto_5$=0, then $\sigma_{h_1}^{\,2} = \sigma_{h_2}^{\,2} = \sigma_{h_3}^{\,2} = \sigma_{h_5}^{\,2} = 0$

$$\sigma_{h_4}^{\,2} = \frac{\propto_4}{2\pi}\int_{-\infty}^{\infty} \frac{\left[\omega^4 - \omega^2 \frac{\beta^2(\alpha-\sigma\alpha)^2}{N^2} S^* L^*\right]^2}{\left[i\omega^5 - i\omega^3 \frac{\beta^2(\alpha-\sigma\alpha)^2}{N^2} S^* L^*\right]^2} d\omega \quad (3.33)$$

If $\propto_1$=$\propto_2$=$\propto_4$=$\propto_5$=0, then $\sigma_{h_4}^{\,2} = \sigma_{h_5}^{\,2} = 0$

$$\sigma_{h_1}^{\,2} = \frac{\propto_3}{2\pi}\int_{-\infty}^{\infty} \frac{\left[\frac{(\alpha-\sigma\alpha)}{N} S^* i\omega^3\right]^2}{\left[i\omega^5 - i\omega^3 \frac{\beta^2(\alpha-\sigma\alpha)^2}{N^2} S^* L^*\right]^2} d\omega \quad (3.34)$$

$$\sigma_{h_2}^{\,2} = \frac{\propto_3}{2\pi}\int_{-\infty}^{\infty} \frac{\left[\frac{\beta(\alpha-\sigma\alpha)^2}{N^2} S^* L^* \omega^2\right]^2}{\left[i\omega^5 - i\omega^3 \frac{\beta^2(\alpha-\sigma\alpha)^2}{N^2} S^* L^*\right]^2} d\omega \quad (3.35)$$

$$\sigma_{h_3}^{\,2} = \frac{\propto_3}{2\pi}\int_{-\infty}^{\infty} \frac{\left[\omega^4 - \omega^2 \frac{\beta^2(\alpha-\sigma\alpha)^2}{N^2} S^* L^*\right]^2}{\left[i\omega^5 - i\omega^3 \frac{\beta^2(\alpha-\sigma\alpha)^2}{N^2} S^* L^*\right]^2} d\omega \quad (3.36)$$

If $\propto_1$=$\propto_3$=$\propto_4$=$\propto_5$=0, then $\sigma_{h_3}^{\,2} = \sigma_{h_4}^{\,2} = \sigma_{h_5}^{\,2} = 0$

$$\sigma_{h_1}^{\,2} = \frac{\propto_2}{2\pi}\int_{-\infty}^{\infty} \frac{\left[\frac{\beta(\alpha-\sigma\alpha)}{N}S^*\, i\omega^3\right]^2}{\left[i\omega^{\,5} - i\omega^3\frac{\beta^2(\alpha-\sigma\alpha)^2}{N^2}S^*L^*\right]^2}\, d\omega \quad (3.37)$$

$$\sigma_{h_2}^{\,2} = \frac{\propto_2}{2\pi}\int_{-\infty}^{\infty} \frac{\left[\omega^4\right]^2}{\left[i\omega^{\,5} - i\omega^3\frac{\beta^2(\alpha-\sigma\alpha)^2}{N^2}S^*L^*\right]^2}\, d\omega \quad (3.38)$$

If $\propto_2 = \propto_3 = \propto_4 = \propto_5 = 0$, then $\sigma_{h_3}^{\,2} = \sigma_{h_4}^{\,2} = \sigma_{h_5}^{\,2} = 0$

$$\sigma_{h_1}^{\,2} = \frac{\propto_1}{2\pi}\int_{-\infty}^{\infty} \frac{\left[\omega^4\right]^2}{\left[i\omega^{\,5} - i\omega^3\frac{\beta^2(\alpha-\sigma\alpha)^2}{N^2}S^*L^*\right]^2}\, d\omega \quad (3.39)$$

$$\sigma_{h_2}^{\,2} = \frac{\propto_1}{2\pi}\int_{-\infty}^{\infty} \frac{\left[-\frac{\beta(\alpha-\sigma\alpha)}{N}L^*\, i\omega^3\right]^2}{\left[i\omega^{\,5} - i\omega^3\frac{\beta^2(\alpha-\sigma\alpha)^2}{N^2}S^*L^*\right]^2}\, d\omega \quad (3.40)$$

This shows the unsteadiness of the population when the population variance is large.

4. Numerical simulations

In this section, we are analysing the steadiness of the system (2.1) in terms of graphs using MATLAB

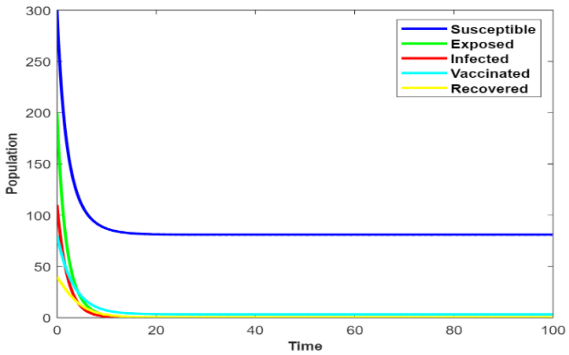

Fig. 1

Fig. 1: The assessment of population fluctuations over time, illustrating the attribute values outlined in Table 1 and the initial values are 300; 200; 110; 80; 30.

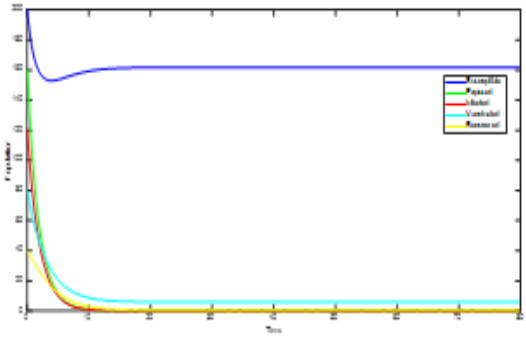

Fig. 2

Fig. 2: The assessment of population fluctuations over time, illustrating the attribute values outlined in Table 1 with r_0=2 and the initial values are 200; 160; 120; 80; 40.

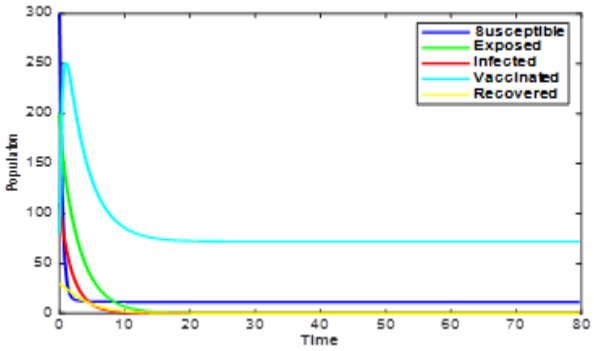

Fig. 3

Fig. 3: The assessment of population fluctuations over time, illustrating the attribute values outlined in Table 1with *A*=25; r_0=2 and the initial values are 300; 200; 110; 80; 30.

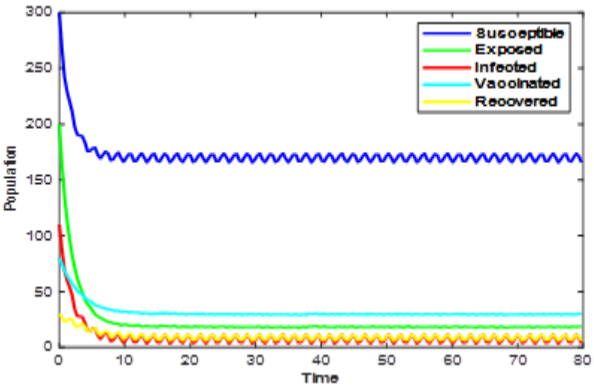

Fig. 4

Fig. 4: Projects the impact of noise intensities on populace classes (Susceptible, Exposed, Infected, Vaccinated, Recovered) at noise values – [15; 12; 15; 12; 10].

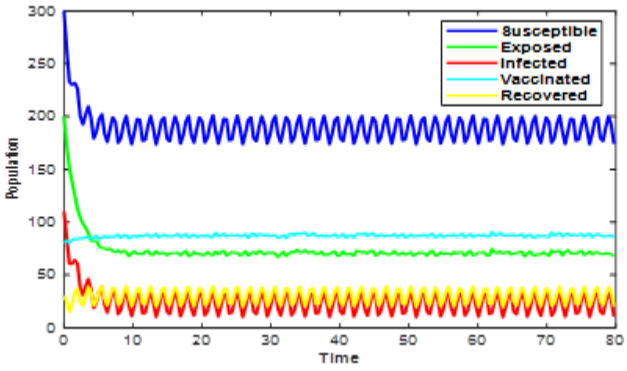

Fig. 5

Fig. 5: Projects the impact of noise intensities on populace classes (Susceptible, Exposed, Infected, Vaccinated, Recovered) at noise values – [50; 45; 45; 40; 35].

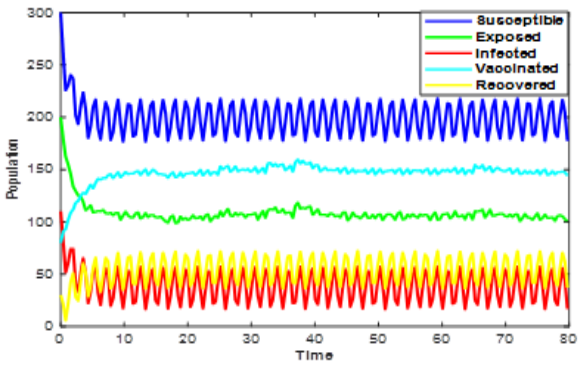

Fig. 6

Fig. 6: Projects the impact of noise intensities on populace classes (Susceptible, exposed, Infected, Vaccinated, Recovered) at noise values – [75; 70; 75; 70; 65]

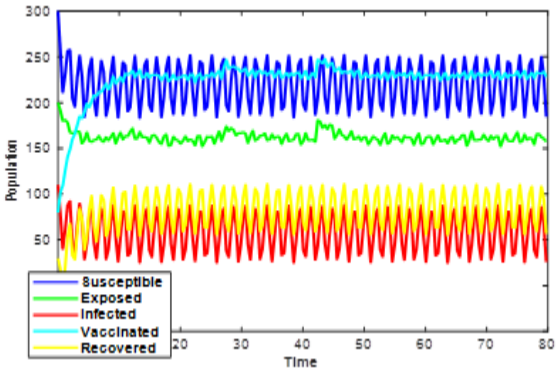

Fig. 7

Fig. 7: Projects the impact of noise intensities on populace classes (susceptible, exposed, Infected, Vaccinated, Recovered) at noise values – [125; 110; 125; 110; 100].

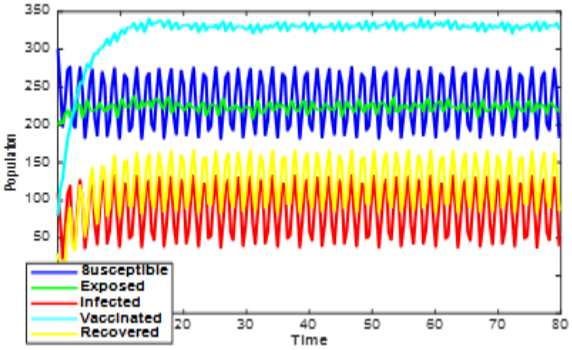

Fig. 8

Fig. 8: Projects the impact of noise intensities on populace classes (Susceptible, exposed, Infected, Vaccinated, Recovered) at noise values – [175; 160; 175; 160; 150].

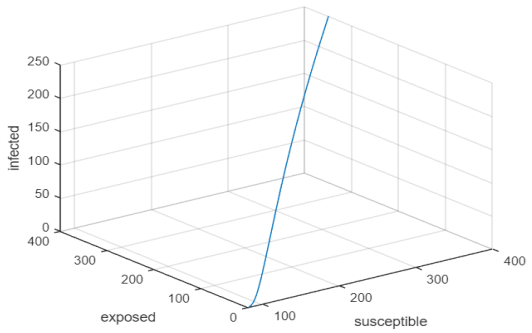

Fig. 9

Fig. 9: Represents a phase portrait of the populations Susceptible-Exposed-Infected with the parameters outlined in Table 1 using initial values 400;350;250;200;100.

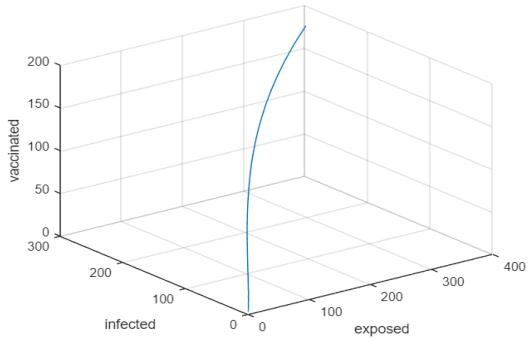

Fig. 10

Fig. 10: Represents a phase portrait of the populations Exposed-Infected-Vaccinated with the parameters of Table 1 using initial values 400;350;250;200;100.

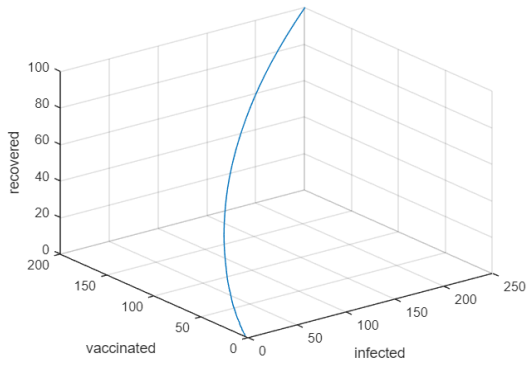

Fig. 11

Fig. 11: Represents a phase portrait of the populations Infected-Vaccinated-Recovered with the parameters of Table 1 using initial values 400;350;250;200;100.

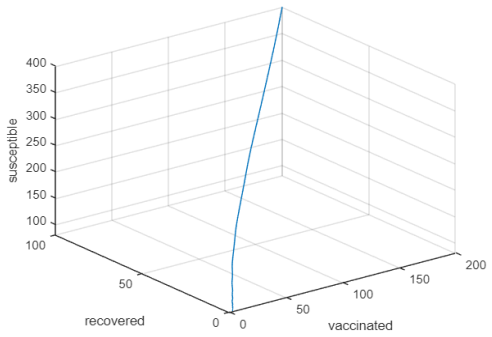

Fig. 12

Fig. 12: Represents a phase portrait of the populations Vaccinated-Recovered-Susceptible with the parameters of Table 1 using initial values 400;350;250;200;100.

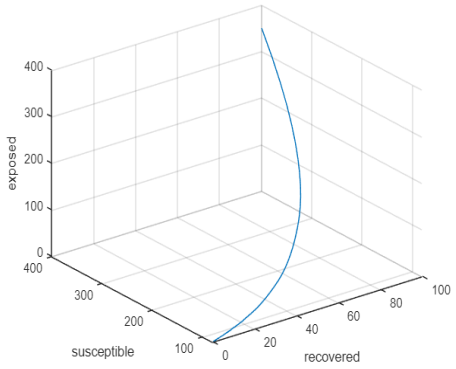

Fig. 13

Fig. 13: Represents a phase portrait of the populations Recovered-Susceptible-Exposed with the parameters of Table 1 using initial values 400;350;250;200;100.

We have modelled a SLIVR system with noise to determine the stability of the population and supported it with the help of graph generated using MATLAB. The observation on the work is given below:

From numerical calculation it is observed that increases in variance leads to instability of the population. In numerical simulations, Fig.1, Fig.2, Fig.3 represent the time population relation without noise. From Fig.2 it is observed that the effect on population recruitment rate(A) affects the stability. Increased recruitment rate with a stable population may lead to the collapse of population stability. From Fig.3 it is noted that as the number of vaccinated people is increased, the exposed population is decreased and the rate of recovery is increased, and the population gets stable. From the analysis, it is also observed that as the effective contact rate and relative transmissibility rate increases, the steadiness of the population is disturbed, and it becomes unstable.

In Fig 4-8, the effects of white noise on the stability of the SLIVR system is visualised. From the graph it is analysed that there is large variation of oscillation about the equilibrium point, which represents that our system is periodic. The amplitude of oscillation is magnified as the intensity of noise is increased. This concludes the role of environmental fluctuation in the stability of our SLIVR model.

5. CONCLUDING REMARKS AND OBSERVATIONS

This paper delves into the SLIVR mathematical framework applied to COVID-19, incorporating white noise as a factor in the analysis. A system where the interaction between susceptible-exposed-infected-vaccinated-recovered populations is created and solved to understand the stability and the role of quarantine measures like isolation and vaccination in the control of pandemic. Both numerical and analytical results emphasize the importance of population variances in understanding system stability. From the model it is observed that as the population exposed increases the larger population gets infected and the population stability is disturbed. It is important to maintain contact rate and transmissibility rate low. The better way to achieve this is isolation. The recruitment rate is one of the main factor that affects the stability of the population. Indeed, vaccination measures play a crucial role in controlling the COVID-19 pandemic.

In the presence of noise, the system displays significant oscillations around equilibrium, indicating periodic behaviour. Numerical simulations demonstrate varying trajectories with oscillations of different amplitudes, initially increasing in noise intensity before stabilizing. The study concludes that stochastic perturbations induce

notable changes in the system dynamics, leading to significant environmental fluctuations due to parameter adjustments.

Conflict of interest

There was no relevant conflict of interest regarding this article.

REFERENCES

1. https://www.who.int/emergencies/diseases/novel-coronavirus-2019
2. https://www.who.int/emergencies/diseases/novel-coronavirus-2019/question-and-answers-hub/q-a-detail/coronavirus-disease-covid-19
3. Ahmad, S., Ullah, A., Al-Mdallal, Q. M., Khan, H., Shah, K., & Khan, A. Fractional order mathematical modeling of COVID-19 transmission. *Chaos, Solitons & Fractals*, 2020; *139:* 110256. https://doi.org/10.1016/j.chaos.2020.110256.
4. Amine, S., & Farah, E. M. Global stability of HIV-1 and HIV-2 model with drug resistance compartment. *Commun. Math. Biol. Neurosci*, *2021*, Article-ID.https://doi.org/10.28919/cmbn/5643.
5. Farah, E. M., Amine, S., Ahmad, S., Nonlaopon, K., & Allali, K. Theoretical and numerical results of a stochastic model describing resistance and non-resistance strains of influenza. *The European Physical Journal Plus*, 2022; *137*(10): 1-15. https://doi.org/10.1140/epjp/s13360-022-03302-5.
6. Nisar, K. S., Ahmad, S., Ullah, A., Shah, K., Alrabaiah, H., & Arfan, M. Mathematical analysis of SIRD model of COVID-19 with Caputo fractional derivative based on real data. *Results in Physics*, 2021; *21*: 103772. https://doi.org/10.1016/j.rinp.2020.103772.
7. Yaagoub, Z., & Allali, K. Fractional HBV infection model with both cell-to-cell and virus-to-cell transmissions and adaptive immunity. *Chaos, Solitons & Fractals*, 2022; *165*: 112855. https://doi.org/10.1016/j.chaos.2022.112855.
8. Din, A., Amine, S., & Allali, A. A stochastically perturbed co-infection epidemic model for COVID-19 and hepatitis B virus. *Nonlinear Dynamics*, 2023; *111*(2): 1921-1945. https://doi.org/10.1007/s11071-022-07899-1.
9. Nainggolan, J., Harianto, J., & Tasman, H. An optimal control of prevention and treatment of COVID-19 spread in Indonesia. *Commun. Math. Biol. Neurosci*, *2023*, Article-ID.https://doi.org/10.28919/cmbn/7820.
10. Amaro, J. E., Dudouet, J., & Orce, J. N. Global analysis of the COVID-19 pandemic using simple epidemiological models. *Applied Mathematical Modelling*, 2021; *90*, 995-1008. https://doi.org/10.1016/j.apm.2020.10.019.
11. Cooper, I., Mondal, A., & Antonopoulos, C. G. A SIR model assumption for the spread of COVID-19 in different communities. *Chaos, Solitons & Fractals*, 2020; *139*, 110057.https://www.ncbi.nlm.nih.gov/pmc/articles/PMC7321055/#:~:text=The%20SIR%20model%20can%20be,individuals%2C%20no%20series%20impacts%20occur
12. Covid map: Coronavirus cases, deaths, vaccinations by country - BBC News
13. Cooper, I., Mondal, A., & Antonopoulos, C. G. A SIR model assumption for the spread of COVID-19 in different communities. *Chaos, Solitons & Fractals*, 2020; *139*: 110057.https://doi.org/10.1016/j.chaos.2020.110057.
14. Lauer, S. A., Grantz, K. H., Bi, Q., Jones, F. K., Zheng, Q., Meredith, H. R, & Lessler, J. (2020). The incubation period of coronavirus disease COVID-19) from publicly reported confirmed cases: estimation and application. *Annals of internal medicine*, 2019; *172*(9): 577-582.https://doi.org/10.7326/m20-0504.
15. He, S., Peng, Y., & Sun, K. SEIR modeling of the COVID-19 and its dynamics. *Nonlinear dynamics*, 2020; *101*: 1667-1680..https://doi.org/10.1007/s11071-020-05743-y.
16. Pandey, G., Chaudhary, P., Gupta, R., & Pal, S. (2020). SEIR and Regression Model based COVID-19 outbreak predictions in India. *arXiv preprint arXiv:2004.00958*.. http://arxiv.org/abs/2004.00958.
17. Rezapour, S., Mohammadi, H., & Samei, M. E. SEIR epidemic model for COVID-19 transmission by Caputo derivative of fractional order. *Advances in difference equations*, *2020;* 1-19. https://doi.org/10.1186%2Fs13662-020-02952-y.
18. Yang, Z., Zeng, Z., Wang, K., Wong, S. S., Liang, W., Zanin, M, & He, J. Modified SEIR and AI prediction of the epidemics trend of COVID-19 in China under public health interventions. *Journal of thoracic disease*, 2020; *12*(3): 165. https://doi.org/10.21037/jtd.2020.02.64.
19. Okuonghae, D., & Omame, A. Analysis of a mathematical model for COVID-19 population dynamics in Lagos, Nigeria. *Chaos, Solitons & Fractals*, 2020; *139*: 110032. https://doi.org/10.1016/j.chaos.2020.110032.
20. Mwalili, S., Kimathi, M., Ojiambo, V., Gathungu, D., & Mbogo, R. SEIR model for COVID-19 dynamics incorporating the environment and social distancing. *BMC Research Notes*, 2020; *13*(1): 352. https://doi.org/10.1186/s13104-020-05192-1
21. Zeb, A., Alzahrani, E., Erturk, V. S., & Zaman, G. Mathematical model for coronavirus disease 2019 (COVID-19) containing isolation class. *BioMed research international*, *2020*. https://www.hindawi.com/journals/bmri/2020/3452402/
22. Zeb, A., Alzahrani, E., Erturk, V. S., & Zaman, G. Mathematical model for coronavirus disease 2019 (COVID-19) containing isolation class. *BioMed research international*, *2020*. https://www.ncbi.nlm.nih.gov/pmc/articles/PMC7327565/

23. Isolation and Precautions for People with COVID-19 | CDC
24. Coronavirus (COVID-19) Vaccinations - Our World in Data
25. Annas, S., Pratama, M. I., Rifandi, M., Sanusi, W., & Side, S. Stability analysis and numerical simulation of SEIR model for pandemic COVID-19 spread in Indonesia. *Chaos, solitons & fractals*, 2020; *139*: 110072.https://doi.org/10.1016/j.chaos.2020.110072 .
26. Ghosh, J. K., Biswas, S. K., Sarkar, S., & Ghosh, U. Mathematical modelling of COVID-19: A case study of Italy. *Mathematics and Computers in Simulation*, 2022; *194:* 1-18. https://www.sciencedirect.com/science/article/pii/S0378475421004043.
27. Amouch, M., & Karim, N. Modeling the dynamic of COVID-19 with different types of transmissions. *Chaos, solitons & fractals*, 2021; *150*: 111188. https://doi.org/10.1016/j.chaos.2021.111188.
28. Hajri, Y., Farah, E. L., Allali, A., & Amine, S. Stability analysis of SLIVR COVID-19 epidemic model with quarantine policy. *Commun. Math. Biol. Neurosci*, *2023*, Article-ID. https://doi.org/10.28919/cmbn%2F8092 .
29. Madhusudanan, V., Srinivas, M. N., & Amalraj, L. Stochastic Analysis of an Epidemic SVIR Model With Holling Type II Incidence and Treatment Rates, 2021. https://doi.org/10.21203/RS.3.RS-603012%2FV1.
30. Ariffin, M. R. K., Gopal, K., Krishnarajah, I., Che Ilias, I. S., Adam, M. B., Arasan, J., & Mohammad Sham, N. Mathematical epidemiologic and simulation modelling of first wave COVID-19 in Malaysia. *Scientific reports*, 2021; *11*(1): 20739. https://doi.org/10.1038/s41598-021-99541-0.
31. Khan, A. A., Ullah, S., & Amin, R. Optimal control analysis of COVID-19 vaccine epidemic model: a case study. *The European Physical Journal Plus*, 2022; *137*(1): 1-25. https://doi.org/10.1140/epjp/s13360-022-02365-8